Electronic Supplementary Material (ESI) for Physical Chemistry Chemical Physics.

Electronic Supplementary Information

Crystalline Structure and Thermotropic Behavior of Alkyltrimethylphosphonium Amphiphiles

Ana Gamarra, Lourdes Urpí, Antxon Martínez de Ilarduya and Sebastián Muñoz-Guerra*

Departament d'Enginyeria Química, Universitat Politècnica de Catalunya, ETSEIB, Diagonal 647, Barcelona 08028, Spain.

E-mail: sebastian.munoz@upc.edu

Contents

Experimental procedures

1. General procedure for the synthesis of trimethylalkylphosphonium salts (*n*ATMP·Br)

2. Methodology used for the single-crystal analysis.

Figures

Fig. SI-1. ^{1}H NMR spectra of *n*ATMP·Br surfactants.

Fig. SI-2. Comparison of FT-IR spectra of *n*ATMP·Br surfactants.

Fig. SI-3. Comparison of the above 0 ºC Krafft temperatures for *n*ATMP·Br and *n*ATMA·Br surfactants (a), plot of the methyl chemical shift of 12ATMP·Br against concentration at 25 ºC with indication of the *cmc*. Inset: evolution of the ^{1}H NMR methyl signal of 12ATMP·Br with concentration (b), and comparison of the *cmc* determined by ^{1}H NMR for *n*ATMP·Br and *n*ATMA·Br with *n*=12, 14 and 16 (c).

Fig. SI-4. a) TGA derivative curves of *n*ATMP·Br surfactants. (b) Isothermal trace of 18ATMP·Br registered at 280 ºC.

Fig. SI-5. TGA traces of *n*ATMA·Br recorded under a nitrogen atmosphere (a) and their corresponding derivative curves (b).

Fig. SI-6. Optical micrograph recorded from the single-crystal of 12ATMP·Br which was obtained by vapor diffusion and used for XRD analysis.

Fig. SI-7. ORTEP representation of the 12ATMP·Br molecule in the conformation adopted in the crystal with atom labelling indication. The displacement ellipsoids are drawn at 50% probability levels and H atoms are drawn as small empty circles of arbitrary radius.

Fig. SI-8. SAXS (left) and WAXS (right) plots from 12ATMP·Br registered over the 10-280 ºC interval. a) heating, b) cooling and c) reheating.

Fig. SI-9. SAXS (left) and WAXS (right) plots from 14ATMP·Br registered over the 0-300 ºC interval. a) heating, b) slow cooling, c) fast cooling and d) reheating.

Fig. SI-10. SAXS (left) and WAXS (right) plots from 16ATMP·Br registered over the 10-280 ºC interval. a) heating, b) cooling and c) reheating.

Fig. SI-11. SAXS (left) and WAXS (right) plots from 18ATMP·Br registered over the 10-280 ºC interval. a) heating, b) cooling and c) reheating.

Fig. SI-12. SAXS (left) and WAXS (right) plots from 20ATMP·Br registered over the 0-300 ºC interval. a) heating, b) slow cooling, c) fast cooling and d) reheating.

Fig. SI-13. SAXS (left) and WAXS (right) plots from 22ATMP·Br registered over the 10-280 ºC interval. a) heating, b) cooling and c) reheating.

Fig. SI-14. Graphical comparison of the observed (at 25 ºC) and calculated main *d*-spacings (nm) with $h \neq 0$ for *n*ATMP·Br.

Fig. SI-15. POM micrographs recorded from *n*ATMP·Br at the indicated temperatures.

Tables

Table SI-1. Crystal data and structure refinement for 12ATMP·Br.

Table SI-2. Atomic coordinates (x 10^4) and equivalent isotropic displacement parameters ($Å^2$ x 10^3) for 12ATMP·Br. U (eq) is defined as one third of the trace of the orthogonalized Uij tensor.

Table SI-3. Torsion angles (º) for 12ATMP·Br.

Table SI-4. Crystallographic *a* and β values of the *n*ATMP·Br salts used for modelling and the crystal lattices from which SAXS and WAXS profiles were simulated.

Contents

Experimental procedures

1. General procedure for the synthesis of trimethylalkylphosphonium salts (*n*ATMP·Br)

1-bromoalkane (5.5 mmol) was placed in a flask immersed into an oil bath (80 ºC) and under a nitrogen atmosphere. After heating for several minutes, the trimethylphosphine (TMP) was slowly added (5 mL, 5 mmol). The mixture was heated up to 116 ºC and stirred for a period of 18 to 24 h depending on the bromoalkane used. The precipitate that appeared upon cooling to room temperature, was collected by filtration, washed several times to remove the excess of alkylbromide, and finally dried under high vacuum.

Dodecyltrimethylphosphonium bromide (12ATMP·Br)

TMP and 1.3 mL of 1-bromododecane gave after 16 h stirring 1.14 g (70%) of the product as a white powder. The chemical structure was ascertained by ^{1}H NMR, ^{13}C NMR, FT-IR and elemental analysis. ^{1} H NMR (300.1 MHz; $CDCl_3$; δ(ppm)): 2.46 (2H, m, RC**H**$_2$P$^+$), 2.25 and 2.20 (9H, d, P$^+$(C**H**$_3$)$_3$), 1.55 (4H, m, RC**H**$_2$C**H**$_2$CH$_2$P$^+$), 1.25 (16H, m, CH$_3$-(C**H**$_2$)$_8$-CH$_2$ CH$_2$P$^+$), 0.88 (3H, t, C**H**$_3$-(CH$_2$)$_{11}$-P$^+$), ^{13} C NMR (75.5 MHz; $CDCl_3$; δ(ppm)): 31.9 (CH$_3$-CH$_2$-**C**H$_2$R), 30.6 (CH$_3$-CH$_2$-CH$_2$-**C**H$_2$R), 30.4-29.0 (CH$_3$-CH$_2$-CH$_2$-(**C**H$_2$)$_5$R), 24.1 (R**C**H$_2$CH$_2$CH$_2$P$^+$), 23.4 (R**C**H$_2$P$^+$), 22.6 (CH$_3$- **C**H$_2$R), 21.8 (R**C**H$_2$-CH$_2$-P$^+$), 14.1 (**C**H$_3$R), 9.4 and 8.6 (P$^+$(**C**H$_3$)$_3$). FT-IR (ν(cm^{-1})): 2913, 2847, 1471, 972, 705. Elemental analysis: C (%): 55.53; found: 55.53, H (%): 10.59; found: 10.50.

Tetradecyltrimethylphosphonium bromide (14ATMP·Br)

TMP and 1.5 mL of 1-bromotetradecane gave after 17 h stirring 1.43 g (80%) of the product as a white powder. The chemical structure was ascertained by ^{1}H NMR, ^{13}C NMR, FT-IR and elemental analysis. ^{1} H NMR (300.1 MHz; $CDCl_3$; δ(ppm)): 2.46 (2H, m, RC**H**$_2$P$^+$), 2.25 and 2.20 (9H, d, P$^+$(C**H**$_3$)$_3$), 1.55 (4H, m, RC**H**$_2$C**H**$_2$CH$_2$P$^+$), 1.25 (20H, m, CH$_3$-(C**H**$_2$)$_{10}$-CH$_2$ CH$_2$P$^+$), 0.88 (3H, t, C**H**$_3$-(CH$_2$)$_{13}$-P$^+$), ^{13} C NMR (75.5 MHz; $CDCl_3$; δ(ppm)): 31.9 (CH$_3$-CH$_2$-**C**H$_2$R), 30.6 (CH$_3$-CH$_2$-CH$_2$-**C**H$_2$R), 30.4-29.0 (CH$_3$-CH$_2$-CH$_2$-(**C**H$_2$)$_7$R), 24.1 (R**C**H$_2$CH$_2$CH$_2$P$^+$), 23.4 (R**C**H$_2$P$^+$), 22.6 (CH$_3$- **C**H$_2$R), 21.8 (R**C**H$_2$-CH$_2$-P$^+$), 14.1 (**C**H$_3$R), 9.4 and 8.6 (P$^+$(**C**H$_3$)$_3$). FT-IR (ν(cm^{-1})): 2911, 2856, 1469, 978, 718. Elemental analysis: C (%): 57.92; found: 58.03, H (%): 10.90; found: 10.79.

Hexadecyltrimethylphosphonium bromide (16ATMP·Br)

TMP and 1.7 mL of 1-bromohexadecane gave after 18 h stirring 1.62 g (85%) of the product as a white powder. The chemical structure was ascertained by ^{1}H NMR, ^{13}C NMR, FT-IR and elemental analysis. ^{1} H NMR (300.1 MHz; $CDCl_3$; δ(ppm)): 2.47 (2H, m, RC**H**$_2$P$^+$), 2.25 and 2.20 (9H, d, P$^+$(C**H**$_3$)$_3$), 1.55 (4H, m, RC**H**$_2$C**H**$_2$CH$_2$P$^+$), 1.25 (24H, m, CH$_3$-(C**H**$_2$)$_{12}$-CH$_2$ CH$_2$P$^+$), 0.88 (3H, t, C**H**$_3$-(CH$_2$)$_{15}$-P$^+$), ^{13} C NMR (75.5 MHz; $CDCl_3$): 31.9 (CH$_3$-CH$_2$-**C**H$_2$R), 30.6 (CH$_3$-CH$_2$-CH$_2$-**C**H$_2$R), 30.4-29.0 (CH$_3$-CH$_2$-CH$_2$-(**C**H$_2$)$_9$R), 24.1 (R**C**H$_2$CH$_2$CH$_2$P$^+$), 23.4 (R**C**H$_2$P$^+$), 22.6 (CH$_3$- **C**H$_2$R), 21.8 (R**C**H$_2$-CH$_2$-P$^+$), 14.1 (**C**H$_3$R), 9.4 and 8.6 (P$^+$(**C**H$_3$)$_3$). FT-IR (ν(cm^{-1})): 2912, 2848, 1472, 981, 716. Elemental analysis: C (%): 59.96; found: 60.06, H (%): 11.16; found: 11.00.

Octadecyltrimethylphosphonium bromide (18ATMP·Br)
TMP and 1.9 mL of 1-bromooctadecane gave after 20 h stirring 1.45 g (70%) of the product as a white powder. The chemical structure was ascertained by ^{1}H NMR, ^{13}C NMR, FT-IR and elemental analysis. ^{1} H NMR (300.1 MHz; $CDCl_3$; δ(ppm)): 2.47 (2H, m, RC**H**$_2$P$^+$), 2.25 and 2.20 (9H, d, P$^+$(C**H**$_3$)$_3$), 1.50 (4H, m, RC**H**$_2$C**H**$_2$CH$_2$P$^+$), 1.26 (28H, m, CH$_3$-(C**H**$_2$)$_{14}$-CH$_2$ CH$_2$P$^+$), 0.88 (3H, t, C**H**$_3$-(CH$_2$)$_{15}$-P$^+$), ^{13} C NMR (75.5 MHz; $CDCl_3$; δ(ppm)): 31.9 (CH$_3$-CH$_2$-**C**H$_2$R), 30.6 (CH$_3$-CH$_2$-CH$_2$-**C**H$_2$R), 30.4-29.0 (CH$_3$-CH$_2$-CH$_2$-(**C**H$_2$)$_{11}$R), 24.1 (R**C**H$_2$CH$_2$CH$_2$P$^+$), 23.4 (R**C**H$_2$P$^+$), 22.6 (CH$_3$- **C**H$_2$R), 21.8 (R**C**H$_2$-CH$_2$-P$^+$), 14.1 (**C**H$_3$R), 9.4 and 8.6 (P$^+$(**C**H$_3$)$_3$). FT-IR (ν(cm^{-1})) : 2915, 2849, 1472, 991, 714. Elemental analysis: C (%): 61.73; found: 61.56, H (%): 11.38; found: 11.22.

Eicosyltrimethylphosphonium bromide (20ATMP·Br)
TMP and 2.0 g of 1-bromoeicosane gave after 22 h stirring 1.7 g (80%) of the product as a white powder. The chemical structure was ascertained by ^{1}H NMR, ^{13}C NMR, FT-IR and elemental analysis. ^{1} H NMR (300.1 MHz; $CDCl_3$; δ(ppm)): 2.47 (2H, m, RC**H**$_2$P$^+$), 2.25 and 2.20 (9H, d, P$^+$(C**H**$_3$)$_3$), 1.50 (4H, m, RC**H**$_2$C**H**$_2$CH$_2$P$^+$), 1.26 (32H, m, CH$_3$-(C**H**$_2$)$_{16}$-CH$_2$ CH$_2$P$^+$), 0.88 (3H, t, C**H**$_3$-(CH$_2$)$_{15}$-P$^+$), ^{13} C NMR (75.5 MHz; $CDCl_3$; δ(ppm)): 31.9 (CH$_3$-CH$_2$-**C**H$_2$R), 30.6 (CH$_3$-CH$_2$-CH$_2$-**C**H$_2$R), 30.4-29.0 (CH$_3$-CH$_2$-CH$_2$-(**C**H$_2$)$_{13}$R), 24.1 (R**C**H$_2$CH$_2$CH$_2$P$^+$), 23.4 (R**C**H$_2$P$^+$), 22.6 (CH$_3$- **C**H$_2$R), 21.8 (R**C**H$_2$-CH$_2$-P$^+$), 14.1 (**C**H$_3$R), 9.4 and 8.6 (P$^+$(**C**H$_3$)$_3$). FT-IR (ν(cm^{-1})): 2915, 2848, 1478, 986, 711. Elemental analysis: C (%): 63.26; found: 63.12, H (%): 11.58; found: 11.37.

Docosyltrimethylphosphonium bromide (22ATMP·Br)
TMP and 2.1 g of 1-bromodocosane gave after 24 h stirring 1.6 g (70%) of the product as a white powder. The chemical structure was ascertained by ^{1}H NMR, ^{13}C NMR, FT-IR and elemental analysis. ^{1} H NMR (300.1 MHz; $CDCl_3$; δ(ppm)): 2.47 (2H, m, RC**H**$_2$P$^+$), 2.25 and 2.20 (9H, d, P$^+$(C**H**$_3$)$_3$), 1.50 (4H, m, R C**H**$_2$C**H**$_2$CH$_2$P$^+$), 1.26 (36H, m, CH$_3$-(C**H**$_2$)$_{18}$-CH$_2$ CH$_2$P$^+$), 0.88 (3H, t, C**H**$_3$-(CH$_2$)$_{15}$-P$^+$), ^{13} C NMR (75.5 MHz; $CDCl_3$; δ(ppm)): 31.9 (CH$_3$-CH$_2$-**C**H$_2$R), 30.6 (CH$_3$-CH$_2$-CH$_2$-**C**H$_2$R), 30.4-29.0 (CH$_3$-CH$_2$-CH$_2$-(**C**H$_2$)$_{15}$R), 24.1 (R**C**H$_2$CH$_2$CH$_2$P$^+$), 23.4 (R**C**H$_2$P$^+$), 22.6 (CH$_3$- **C**H$_2$R), 21.8 (R**C**H$_2$-CH$_2$-P$^+$), 14.1 (**C**H$_3$R), 9.4 and 8.6 (P$^+$(**C**H$_3$)$_3$). FT-IR (ν(cm^{-1})): 2911, 2848, 1474, 989, 716. Elemental analysis: C (%): 64.61; found: 64.70, H (%): 11.75; found: 11.65.

2. Methodology used for the single-crystal analysis

A crystal of 12ATMP·Br was mounted on a D8 Venture diffractometer, the radiation used was from a microfocus with a multilayer monochromator with Mo-Kα radiation (λ = 0.071073 nm), and the diffraction was collected with an area detector Photon 100 CMOS. The unit cell parameters were determined from 7111 reflections (2.23º < θ < 25.14º) and refined by least-squares method. Intensities of 25175 reflections (2.23º < θ < 25.39º) were collected, 3385 of which were unique (R_{int} = 0.0429), and 2530 unique reflections were considered as observed (conditions $I > 2\sigma(I)$). Lorentz-polarization and absorption corrections were made.

The structure was solved by direct methods (SHELXS program) and refined by full-matrix least-squared method (SHELXL-2014 program; G.M. Sheldrick, Acta Cryst. 2015, C71, 3-8).

The minimized function was $\sum w\left|\left|F_0\right|^2 - \left|F_c\right|^2\right|^2$ where

$$w = [\sigma^2(F_0^2) + (0.0390P)^2 + 0.4830P]^{-1} \quad P = (F_0^2 + 2F_c^2)/3 .$$

All H atoms were added with idealized geometry and all C-H bond lengths were refined with the constraint that all C-H distances in a group were equal. For all CH_2 (and CH_3) groups, the H isotropic temperature factor has been calculated equal to 1.2 (and 1.5) times the equivalent temperature factor of the atom to which they are linked. The final *R* factors are shown in Table SI-1 together with other details of the quality of the molecule structure.

Figures

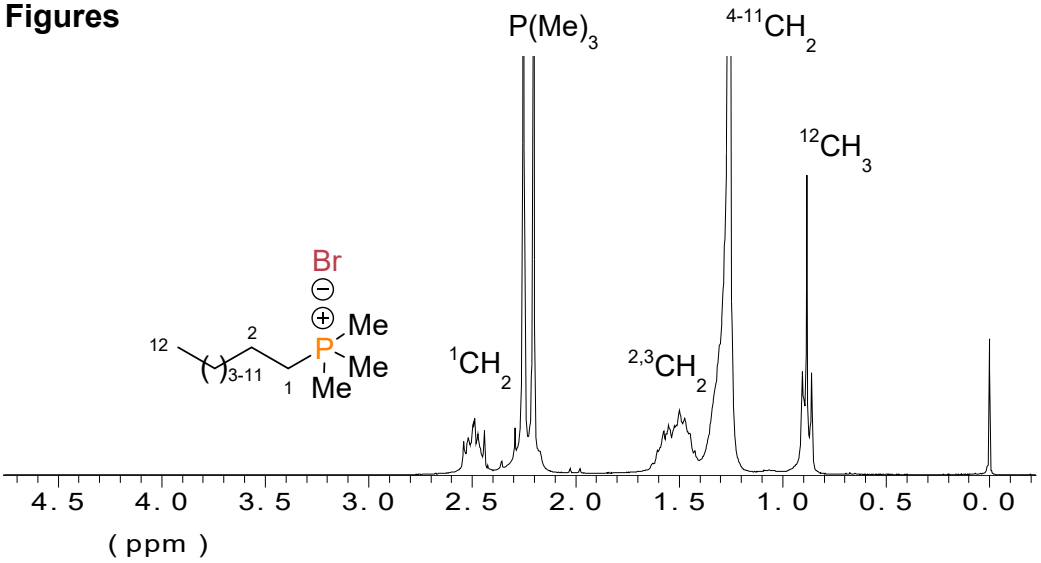
P(Me)3
4-11CH2
12CH3
Br
Me
Me
Me
12
2
3-11
1
1CH2
2,3CH2
4.5 4.0 3.5 3.0 2.5 2.0 1.5 1.0 0.5 0.0
(ppm)

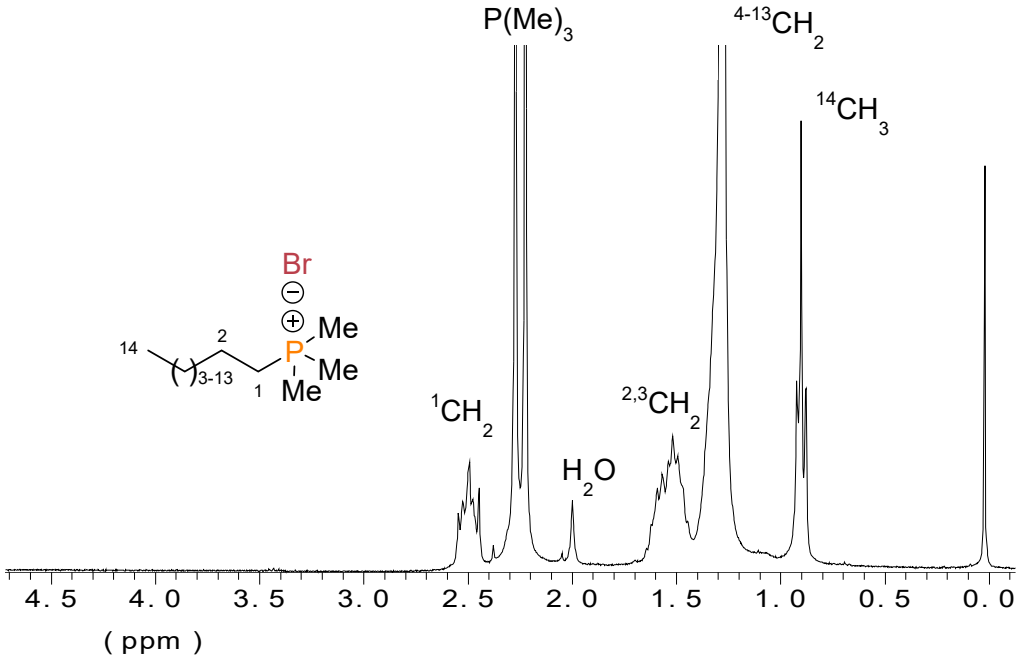
P(Me)3
4-13CH2
14CH3
Br
Me
Me
Me
14
2
3-13
1
1CH2
H2O
2,3CH2
4.5 4.0 3.5 3.0 2.5 2.0 1.5 1.0 0.5 0.0
(ppm)

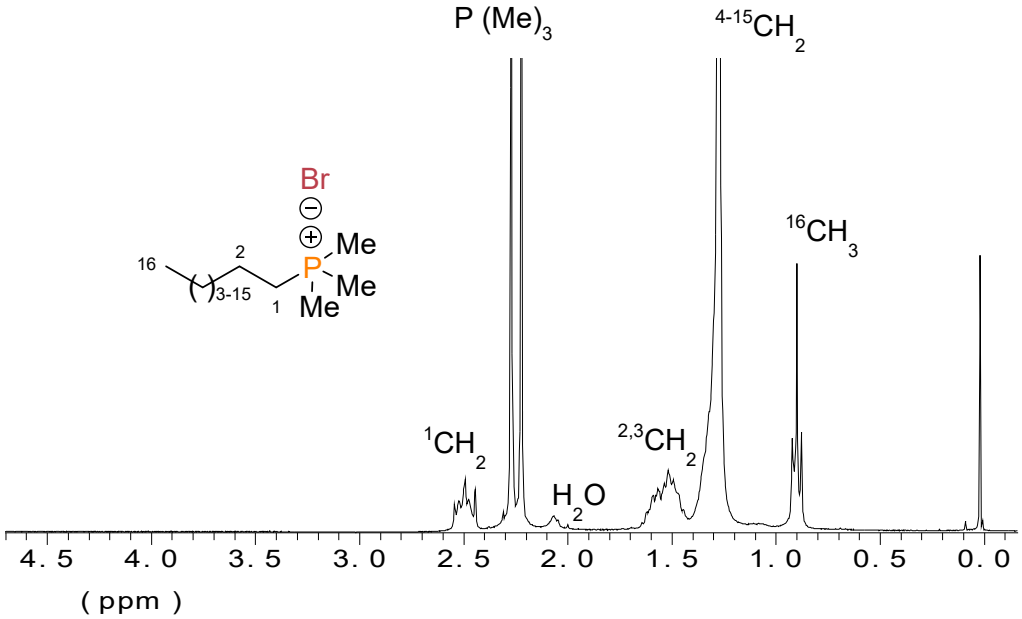
P (Me)3
4-15CH2
16CH3
Br
Me
Me
Me
16
2
3-15
1
1CH2
H2O
2,3CH2
4.5 4.0 3.5 3.0 2.5 2.0 1.5 1.0 0.5 0.0
(ppm)

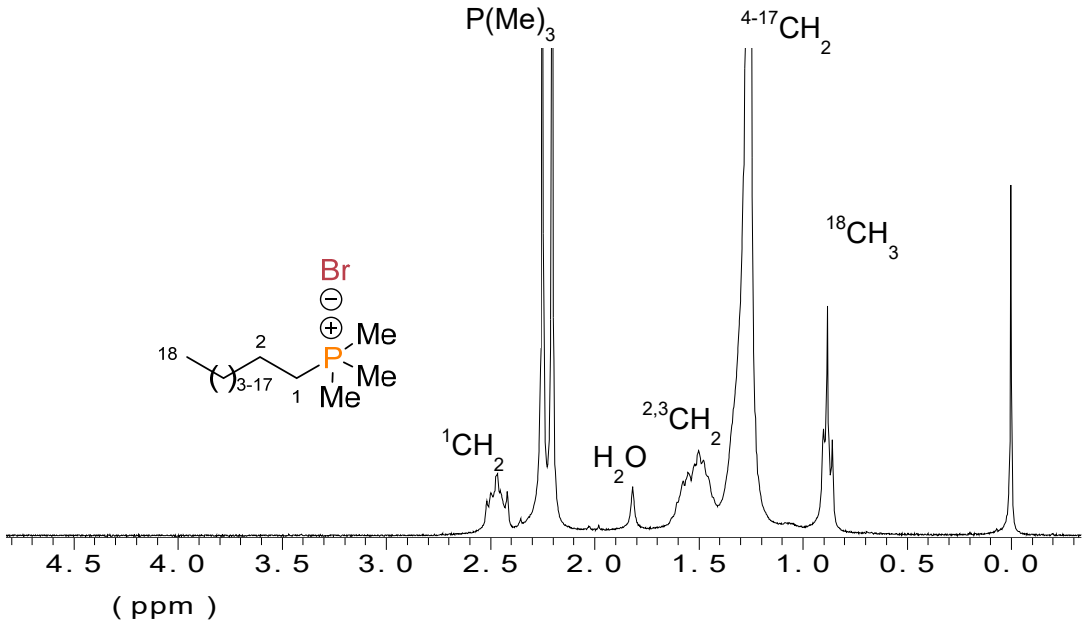

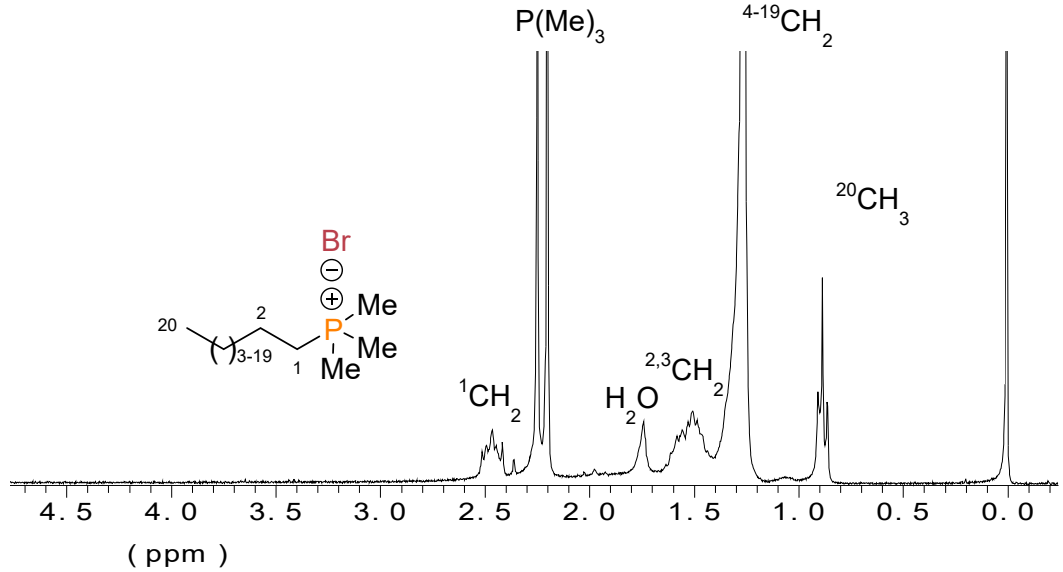

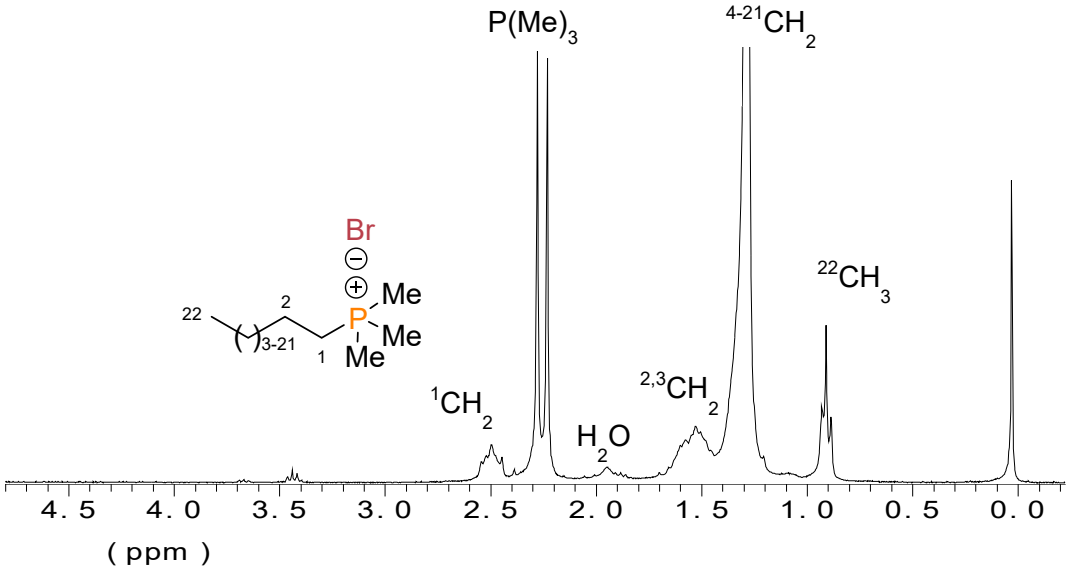

Fig. SI-1. ^{1}H NMR spectra of *n*ATMP·Br surfactants.

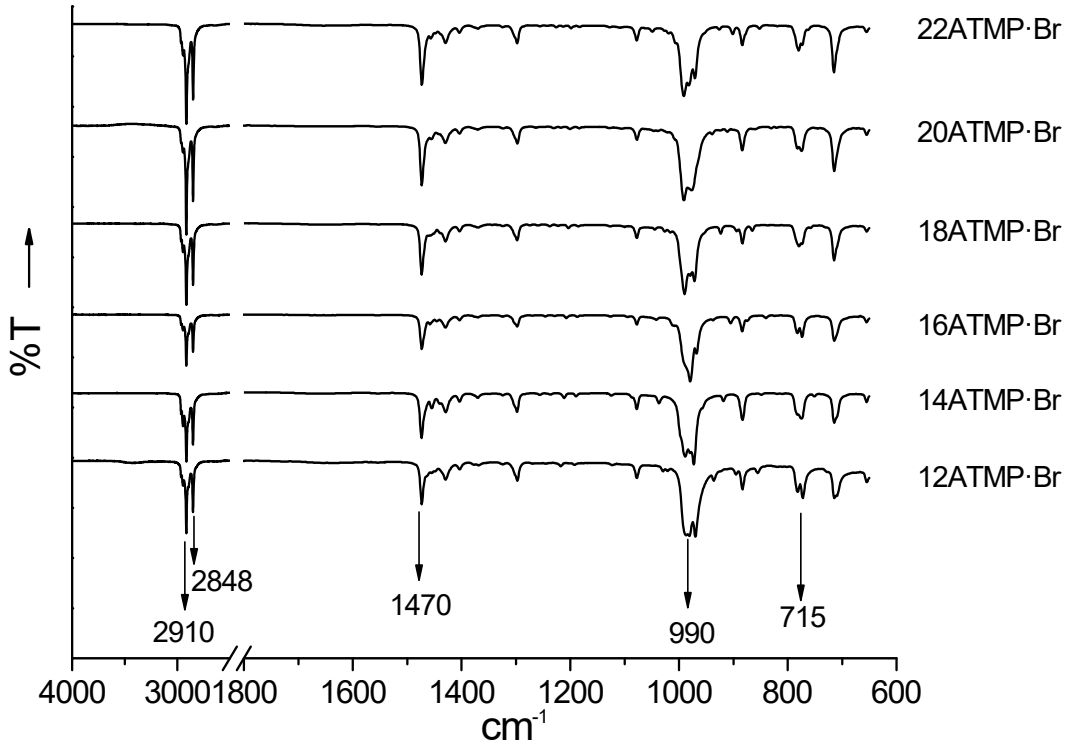

Fig. SI-2. Comparison of FT-IR spectra of *n*ATMP·Br surfactants.

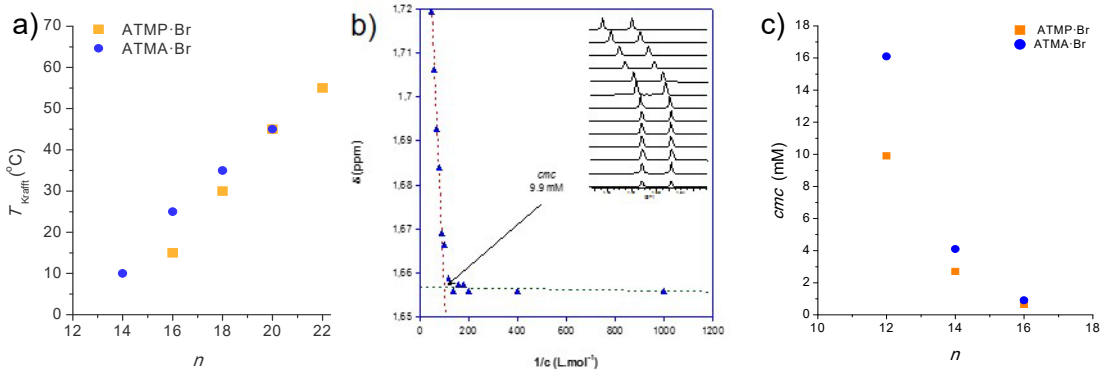

Fig. SI-3. Comparison of the above 0 ºC Krafft temperatures for *n*ATMP·Br and *n*ATMA·Br surfactants (a), plot of the methyl chemical shift of 12ATMP·Br against concentration at 25 ºC with indication of the *cmc*; inset: the evolution of the ^{1}H NMR methyl signal of 12ATMP·Br with concentration (b) and comparison of the *cmc* determined by ^{1}H NMR for *n*ATMP·Br and *n*ATMA·Br with *n*=12, 14 and 16 (c).

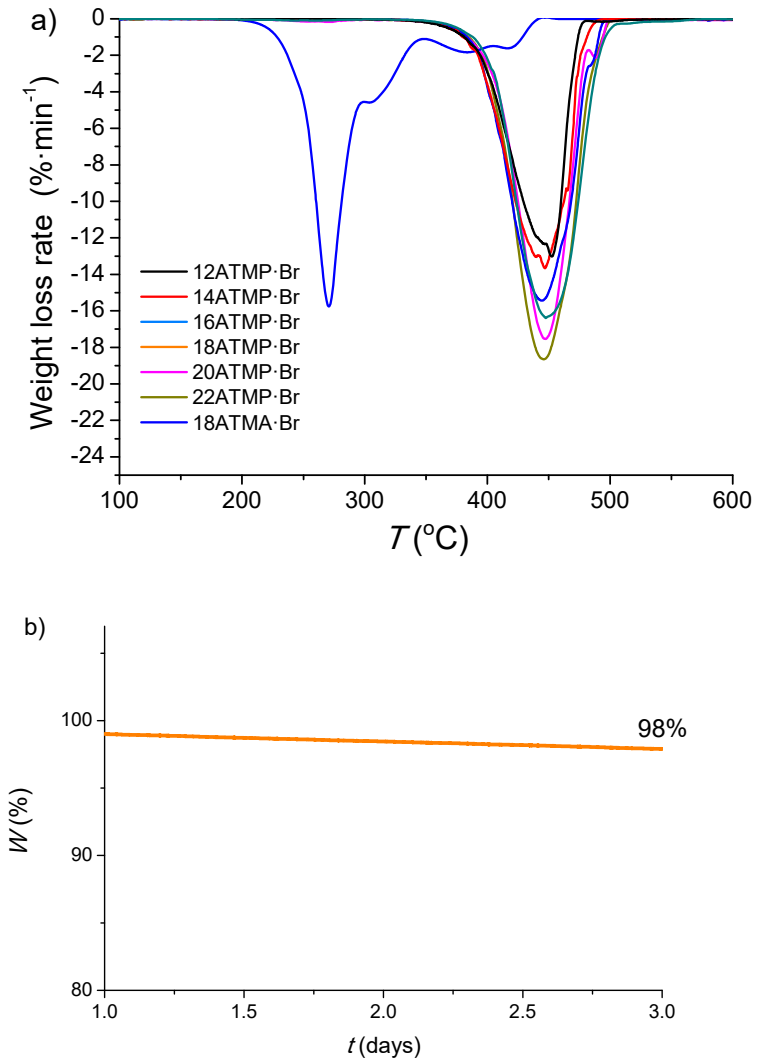

Fig. SI-4. TGA derivative curves of *n*ATMP·Br surfactants (a). Isothermal essay realized with 18ATMP·Br at 280 ºC (b).

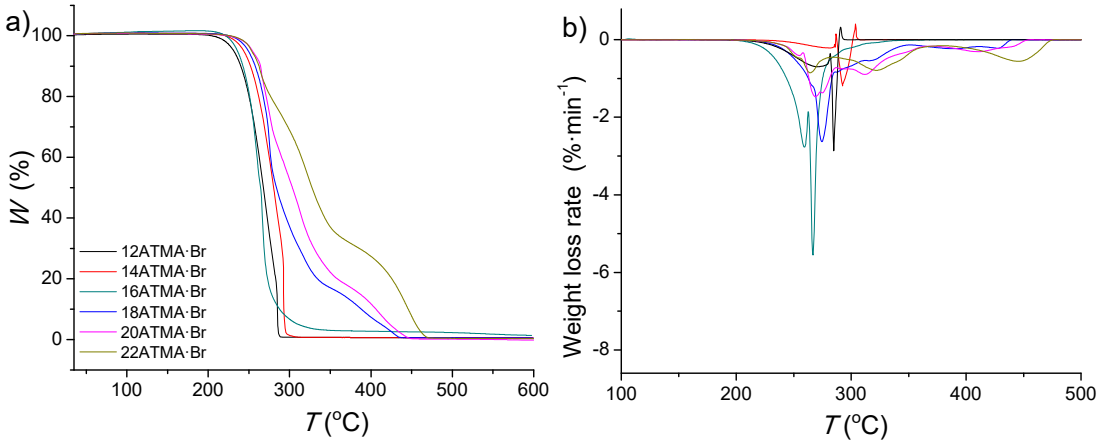

Fig. SI-5. TGA traces of *n*ATMA·Br recorded under a nitrogen atmosphere (a) and their corresponding derivative curves (b).

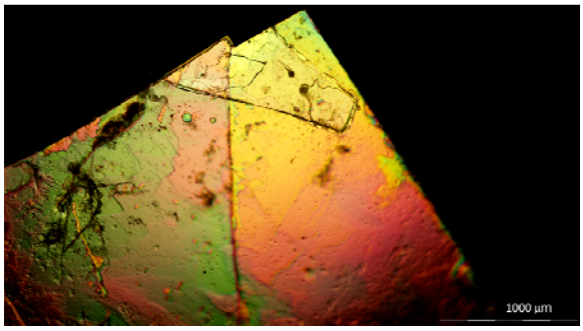

Fig. SI-6. Optical micrograph recorded from the single-crystal of 12ATMP·Br which was obtained by vapor diffusion technique and used for XRD analysis.

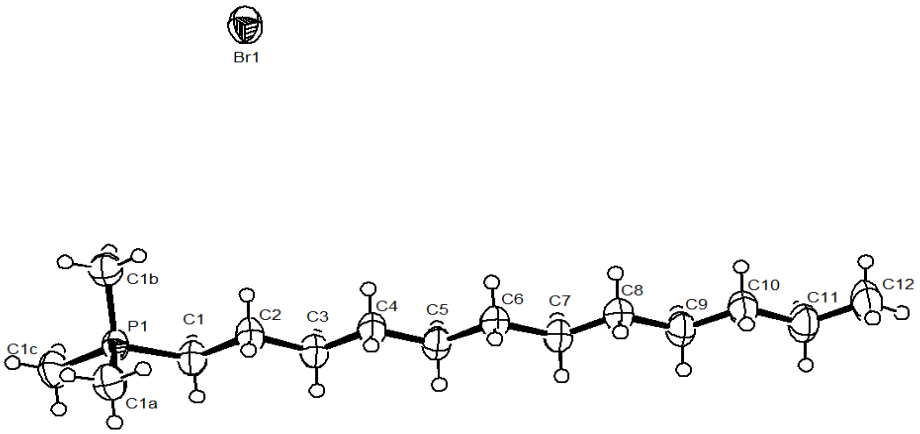

Fig. SI-7. ORTEP representation of the 12ATMP·Br molecule in the conformation adopted in the crystal with atom labelling indication. The displacement ellipsoids are drawn at 50% probability levels and H atoms are drawn as small empty circles of arbitrary radius.

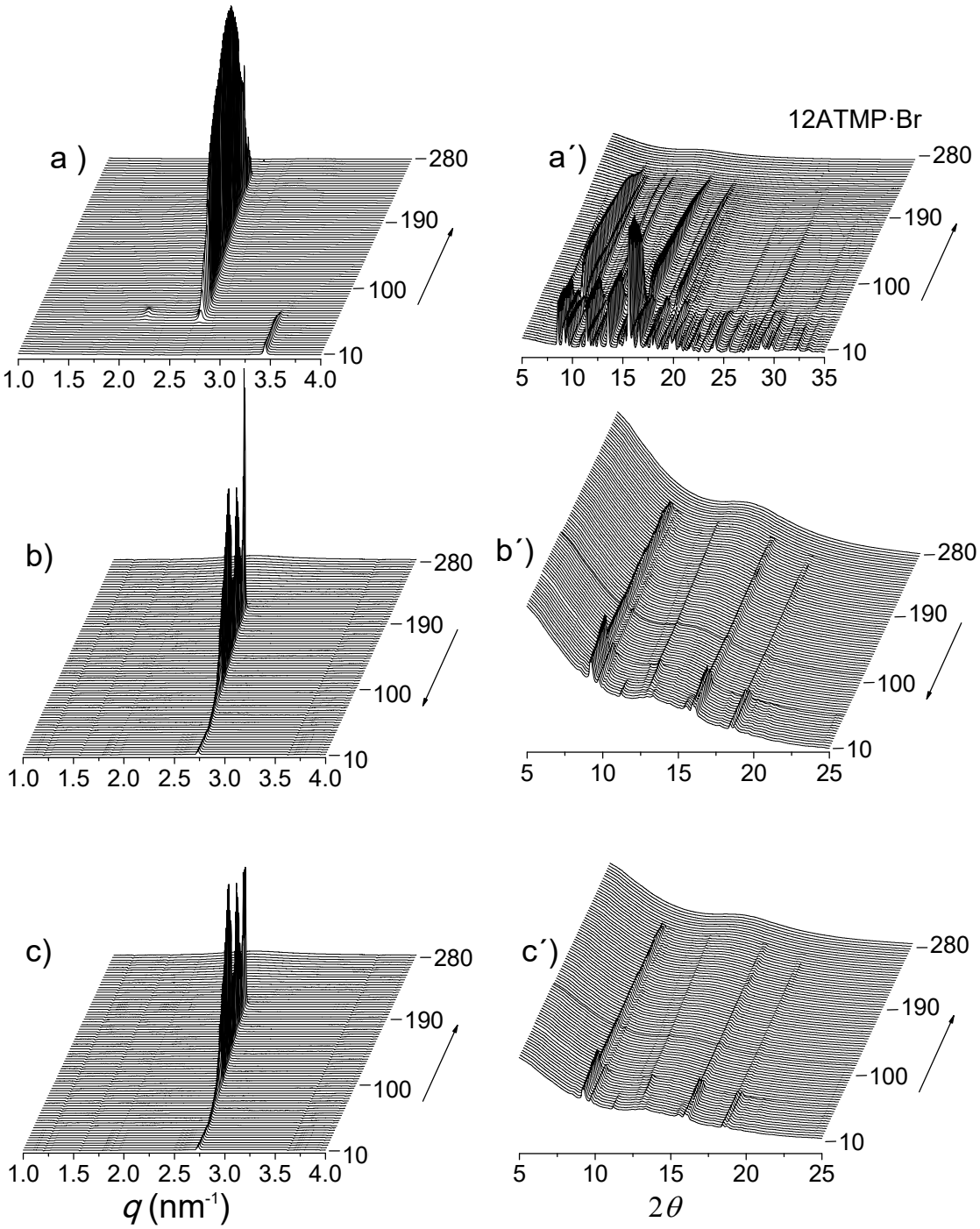

Fig. SI-8. SAXS (left) and WAXS (right) plots from 12ATMP·Br registered over the 10-280 ºC interval. a) heating, b) cooling and c) reheating.

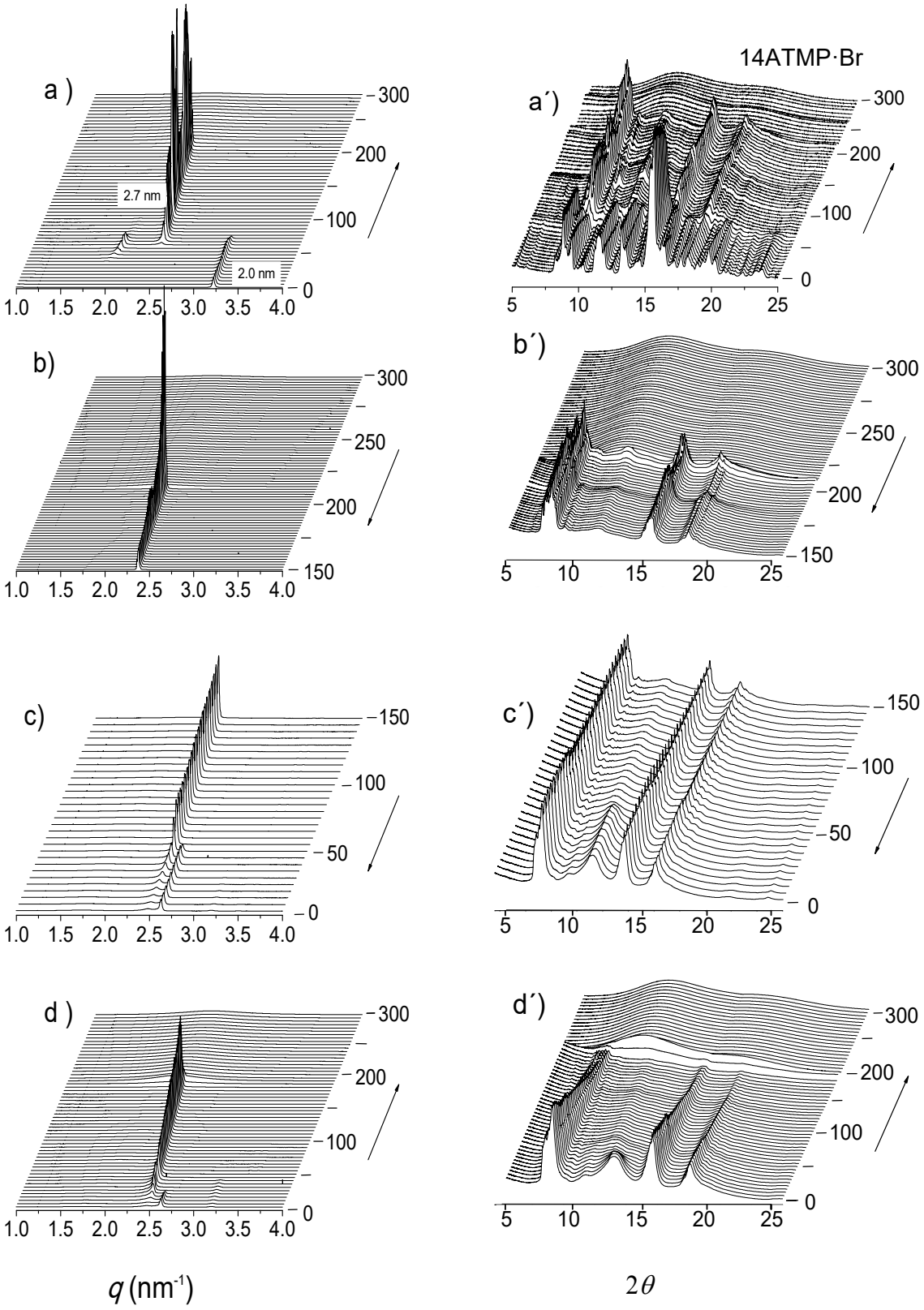

Fig. SI-9. SAXS (left) and WAXS (right) plots from 14ATMP·Br registered over the 0-300 ºC interval. a) heating, b) slow cooling, c) fast cooling and d) reheating.

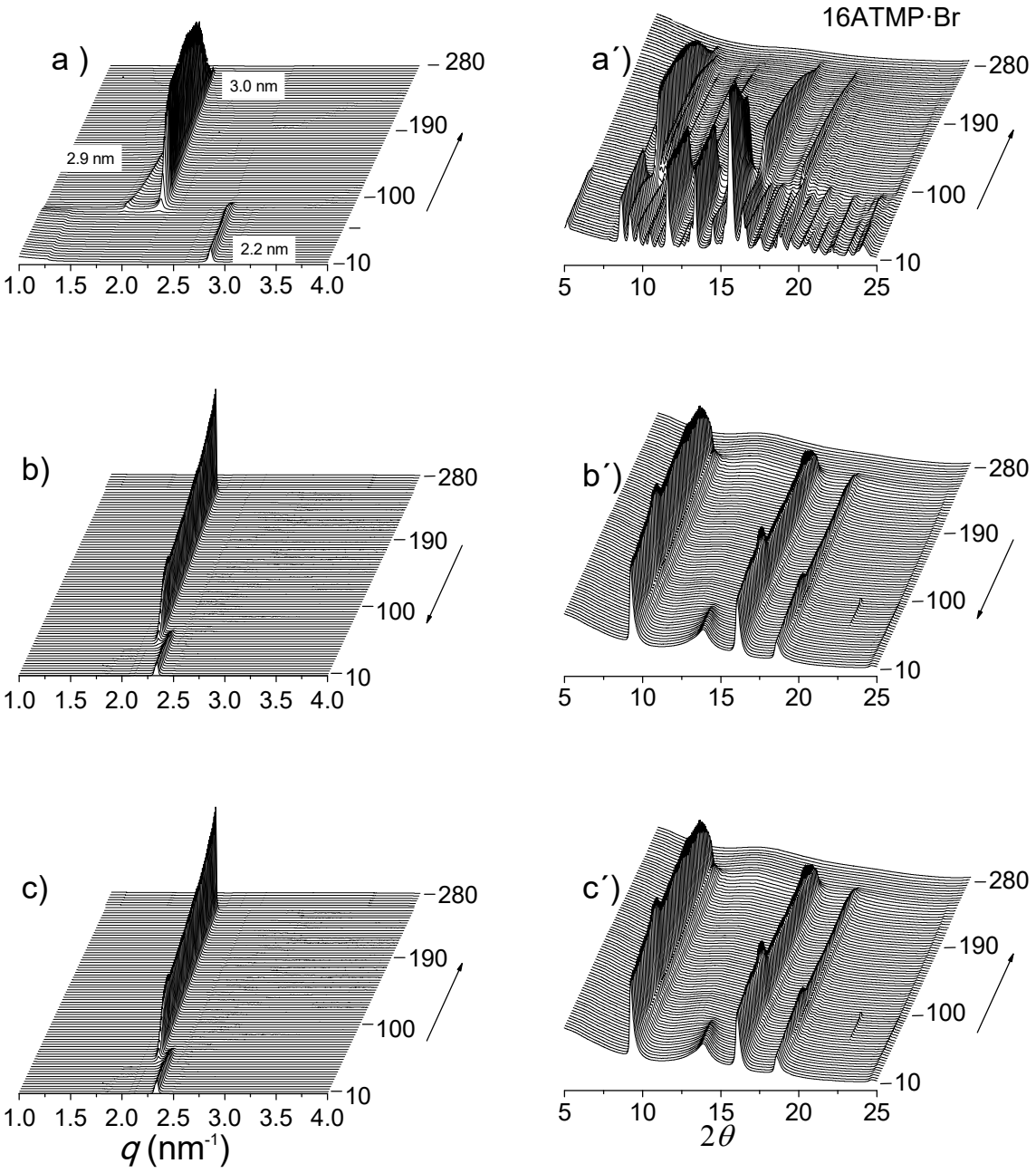

Fig. SI-10. SAXS (left) and WAXS (right) plots from 16ATMP·Br registered over the 10-280 ºC interval. a) heating, b) cooling and c) reheating.

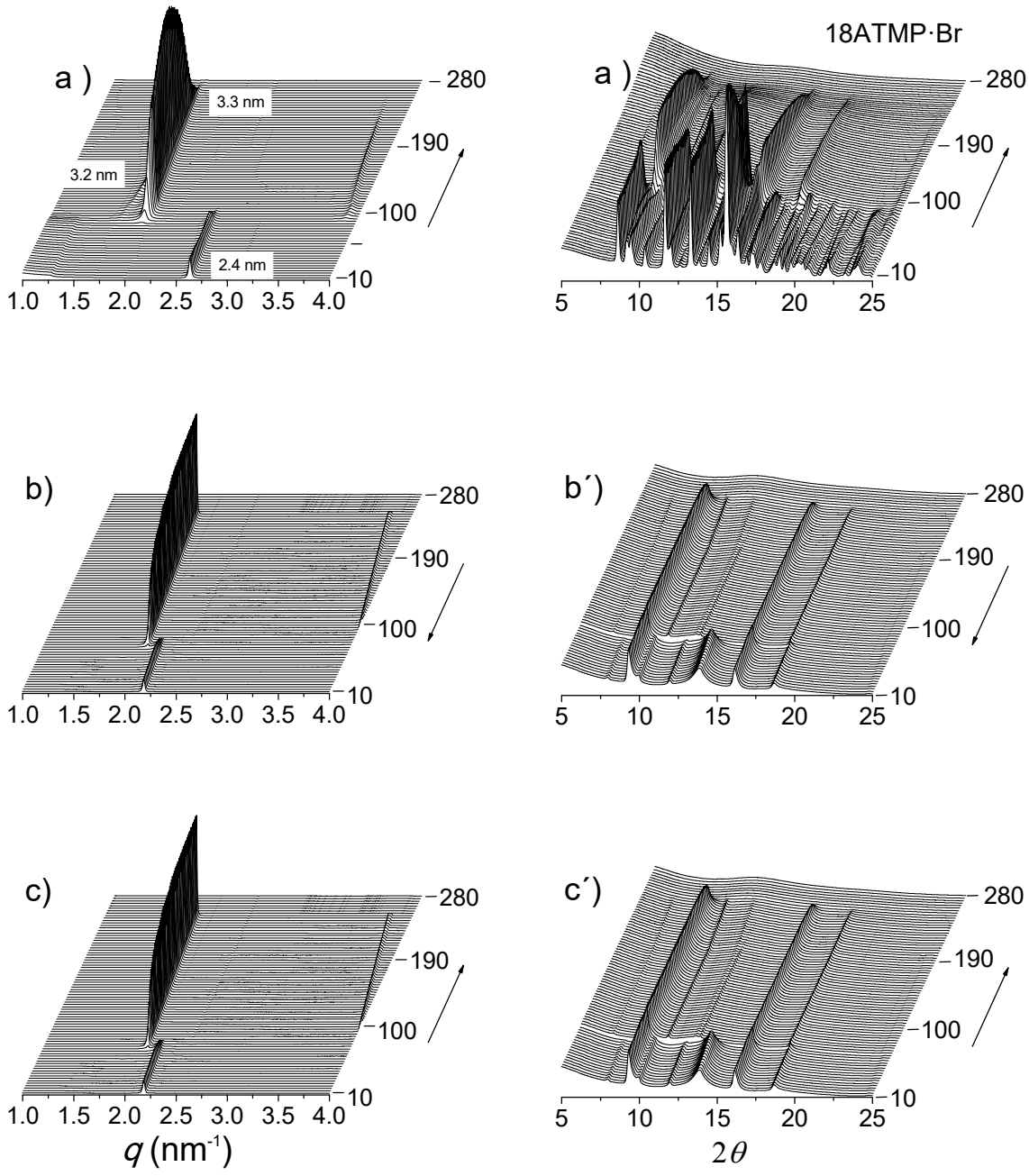

Fig. SI-11. SAXS (left) and WAXS (right) plots from 18ATMP·Br registered over the 10-280 ºC interval. a) heating, b) cooling and c) reheating.

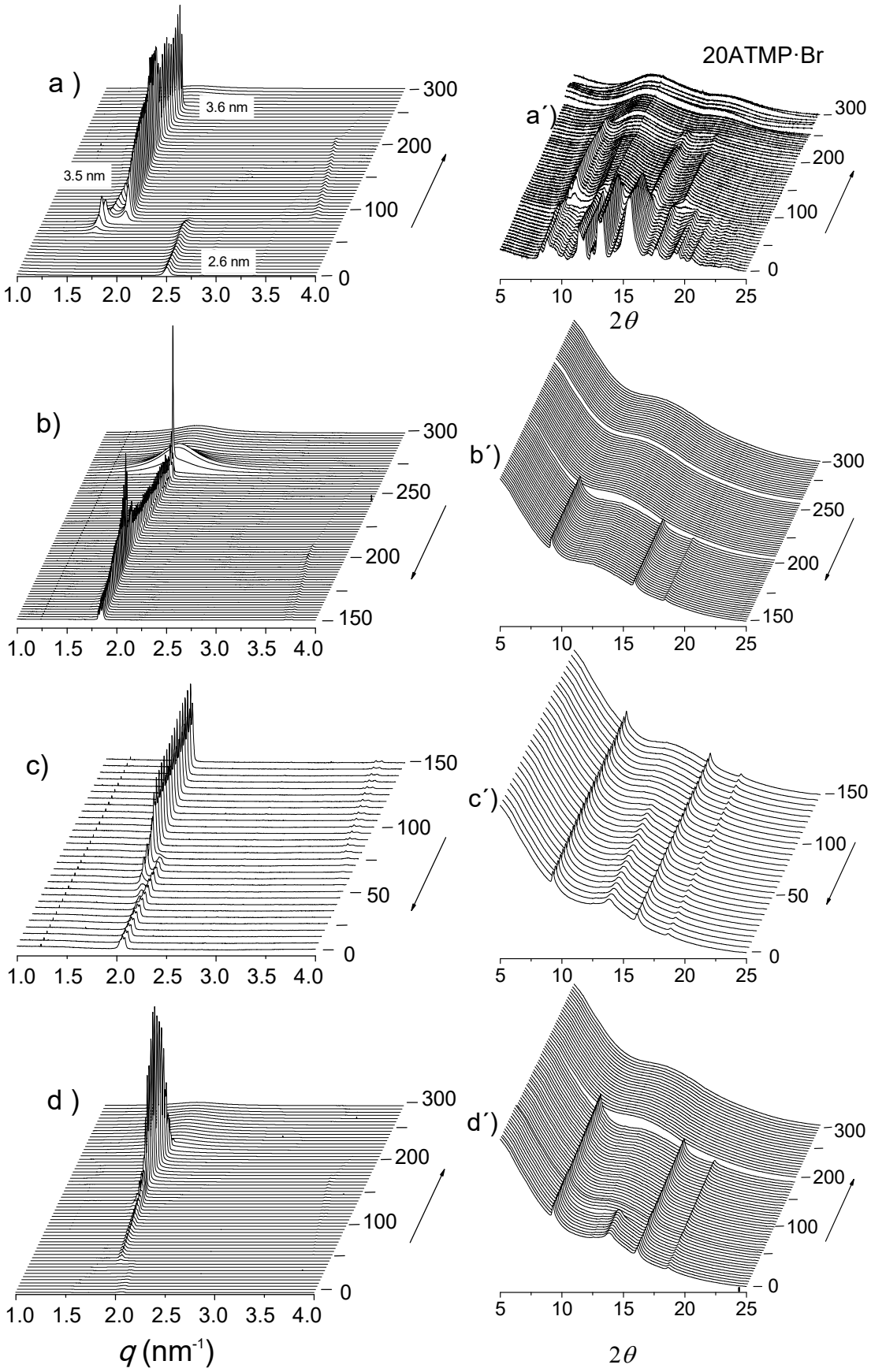

Fig. SI-12. SAXS (left) and WAXS (right) plots from 20ATMP·Br registered over the 0-300 ºC interval. a) heating, b) slow cooling, c) fast cooling and d) reheating.

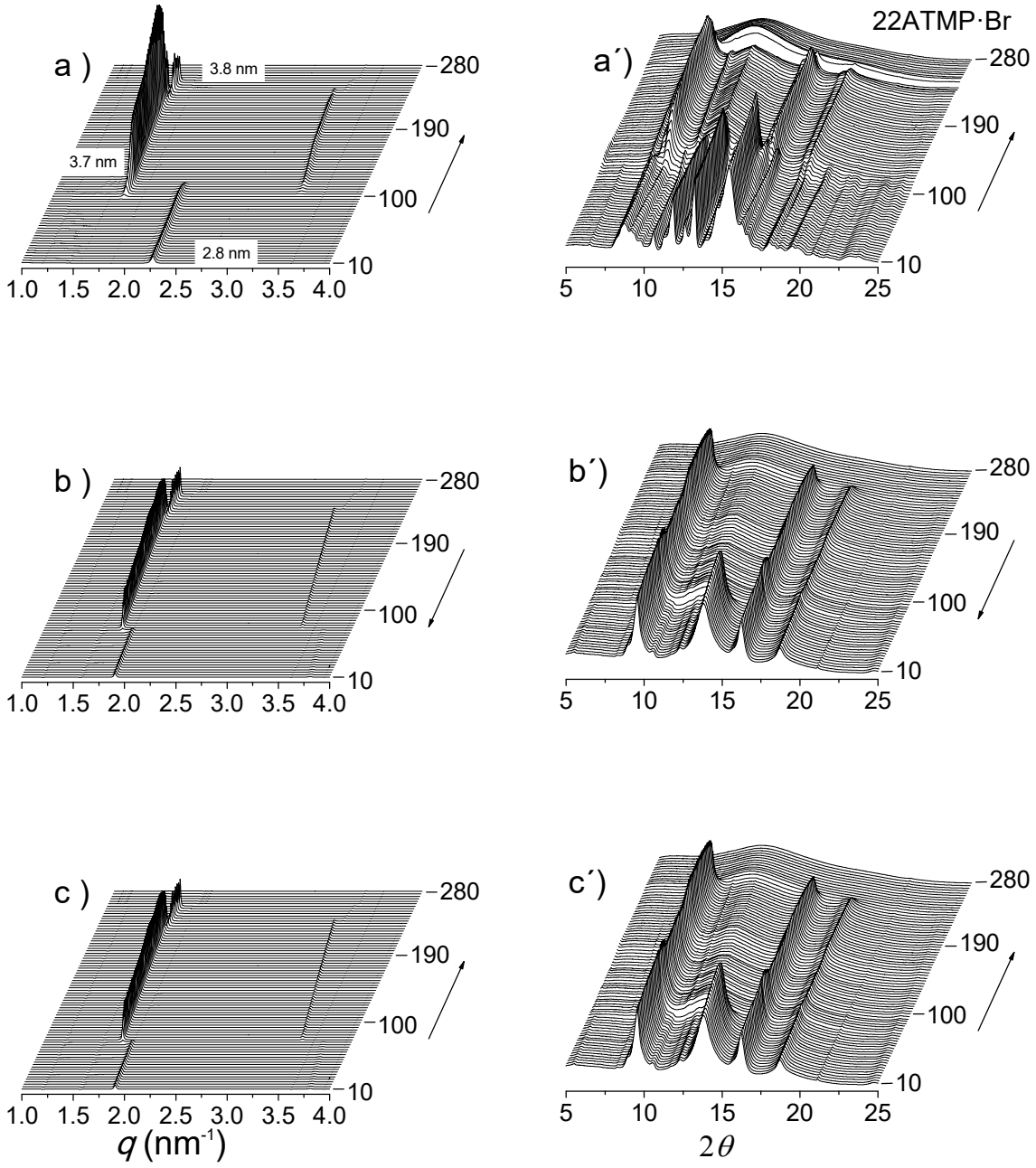

Fig. SI-13. SAXS (left) and WAXS (right) plots from 22ATMP·Br registered over the 10-280 ºC interval. a) heating, b) cooling and c) reheating.

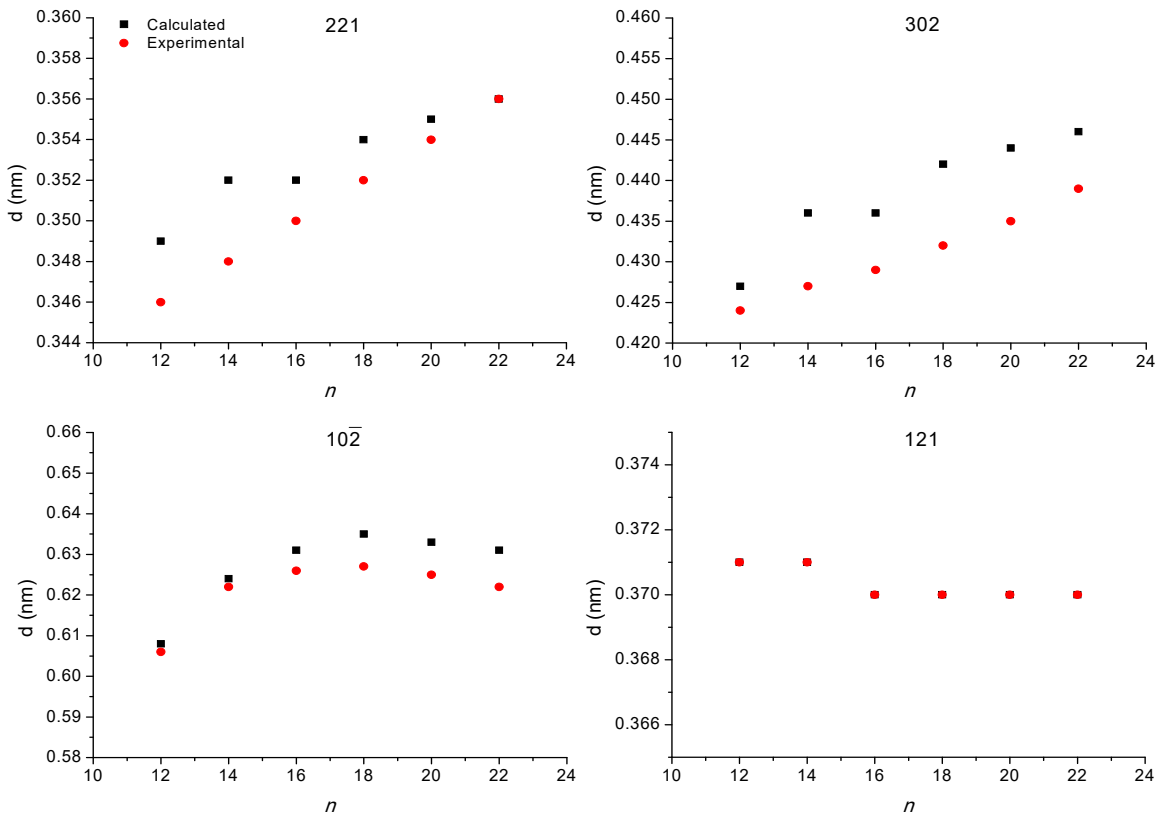

Fig. SI-14. Graphical comparison of the observed (at 25 ºC) and calculated main *d*-spacings (nm) with $h \neq 0$ for *n*ATMP·Br.

12ATMP·Br

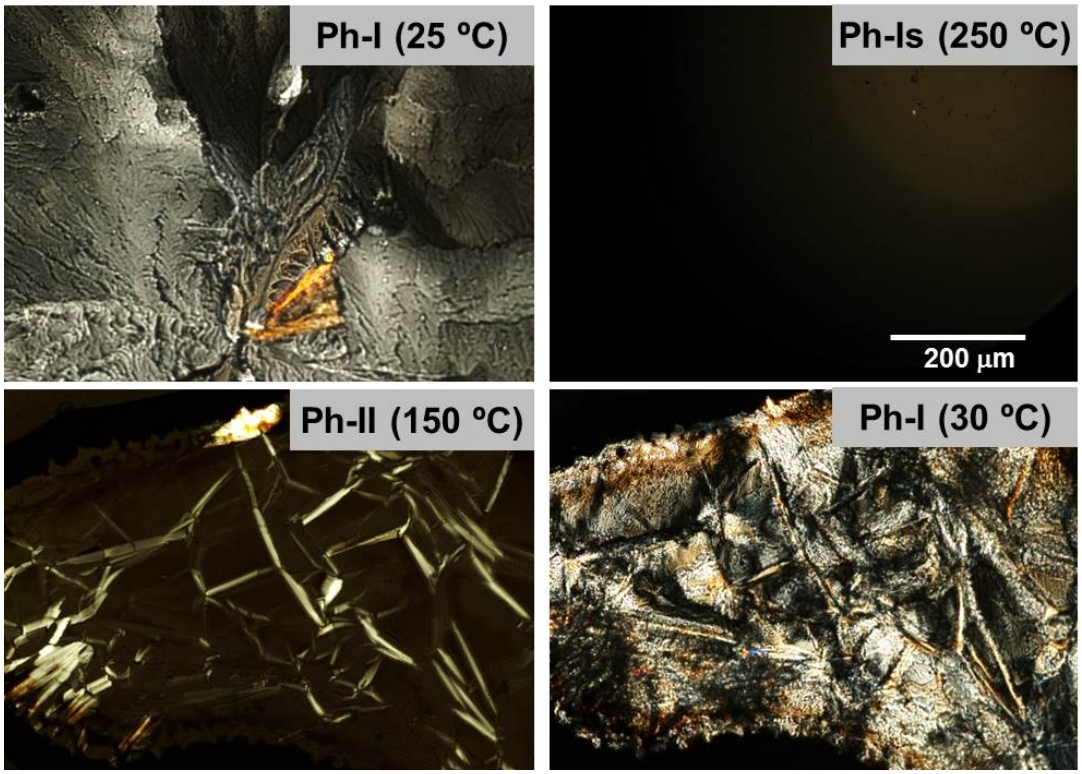

16ATMP·Br

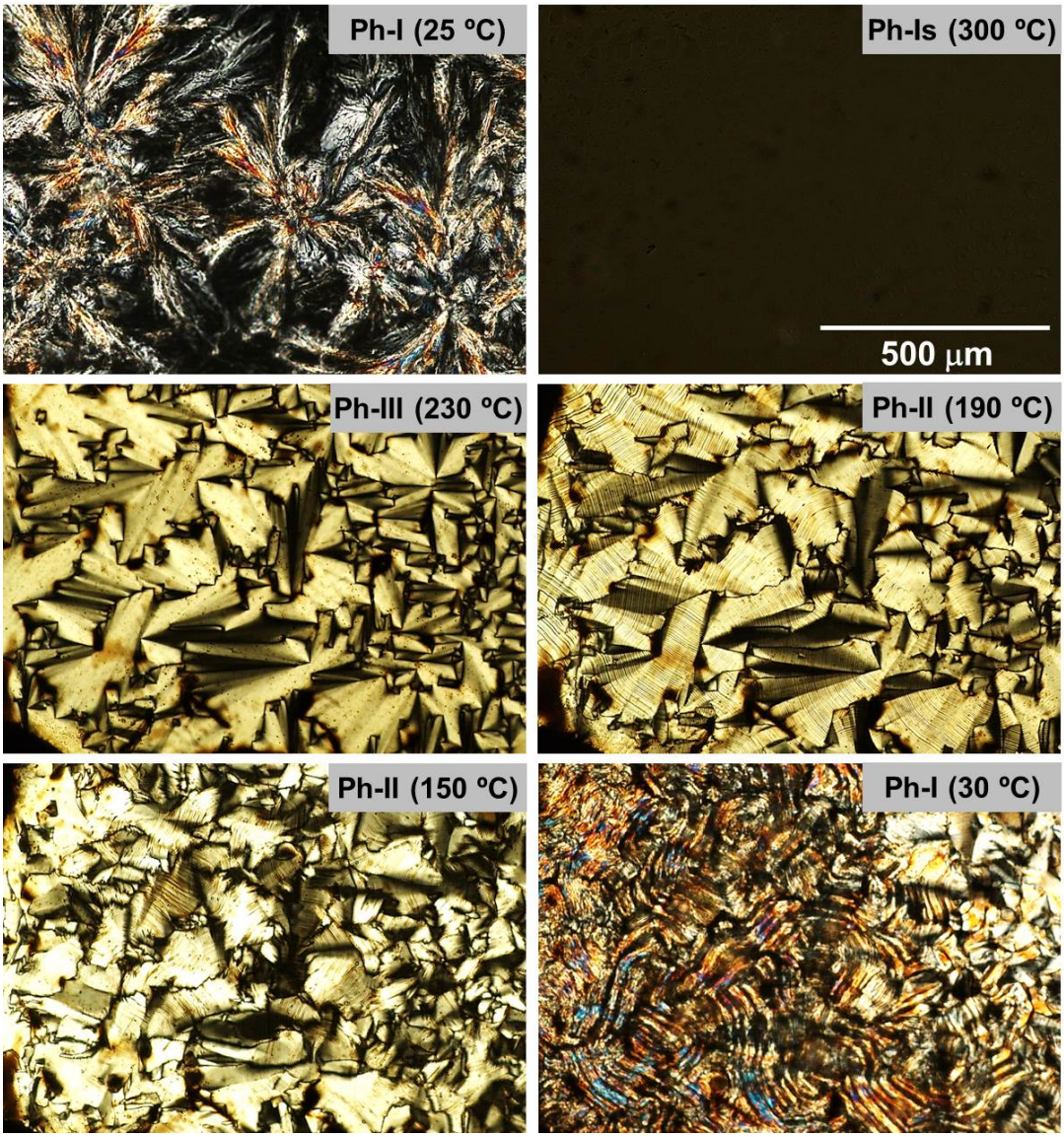
Ph-I (25 ºC)
Ph-Is (300 ºC)
500 μm
Ph-III (230 ºC)
Ph-II (190 ºC)
Ph-II (150 ºC)
Ph-I (30 ºC)

18ATMP·Br

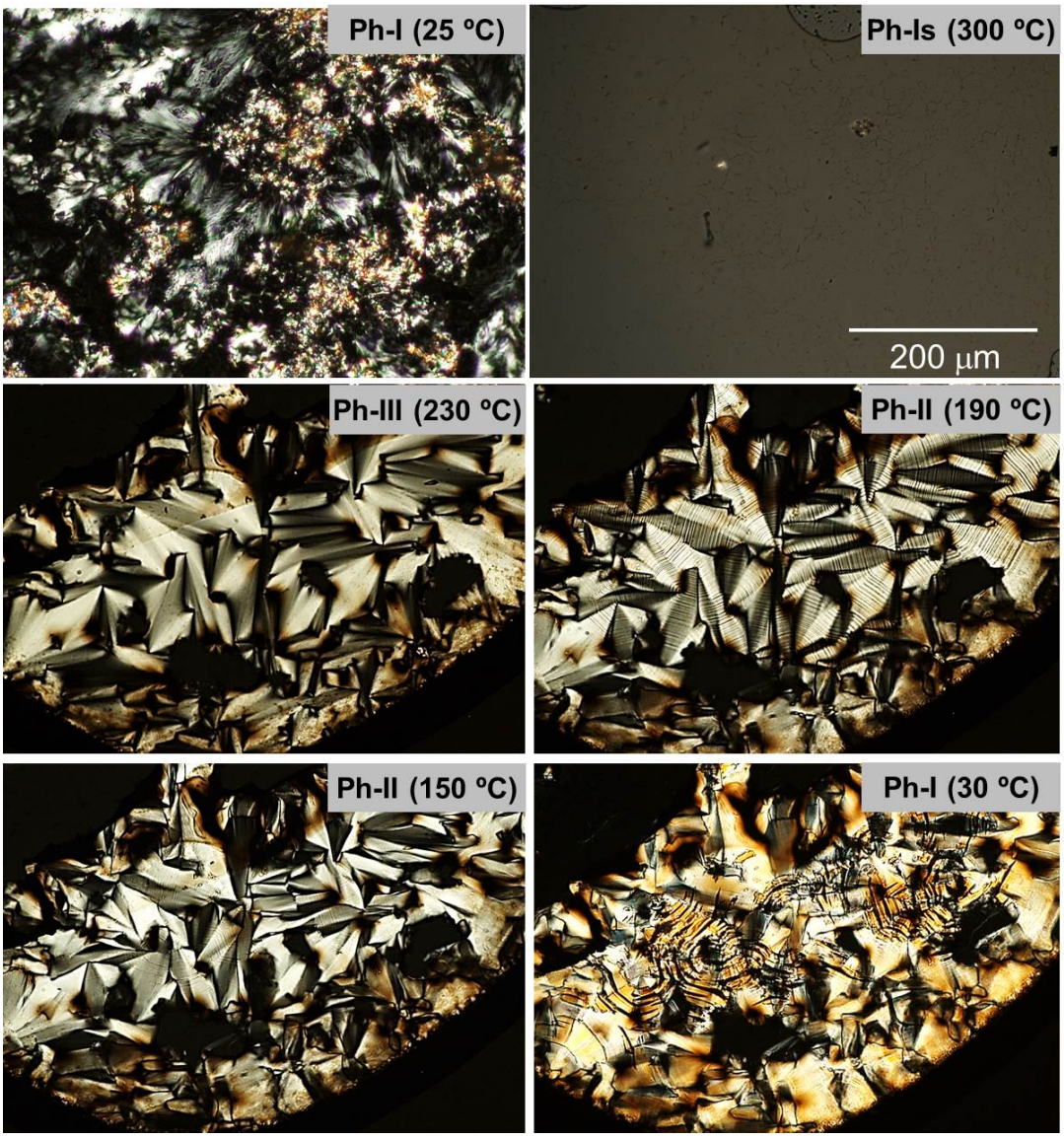
Ph-I (25 ºC)
Ph-Is (300 ºC)
200 μm
Ph-III (230 ºC)
Ph-II (190 ºC)
Ph-II (150 ºC)
Ph-I (30 ºC)

22ATMP·Br

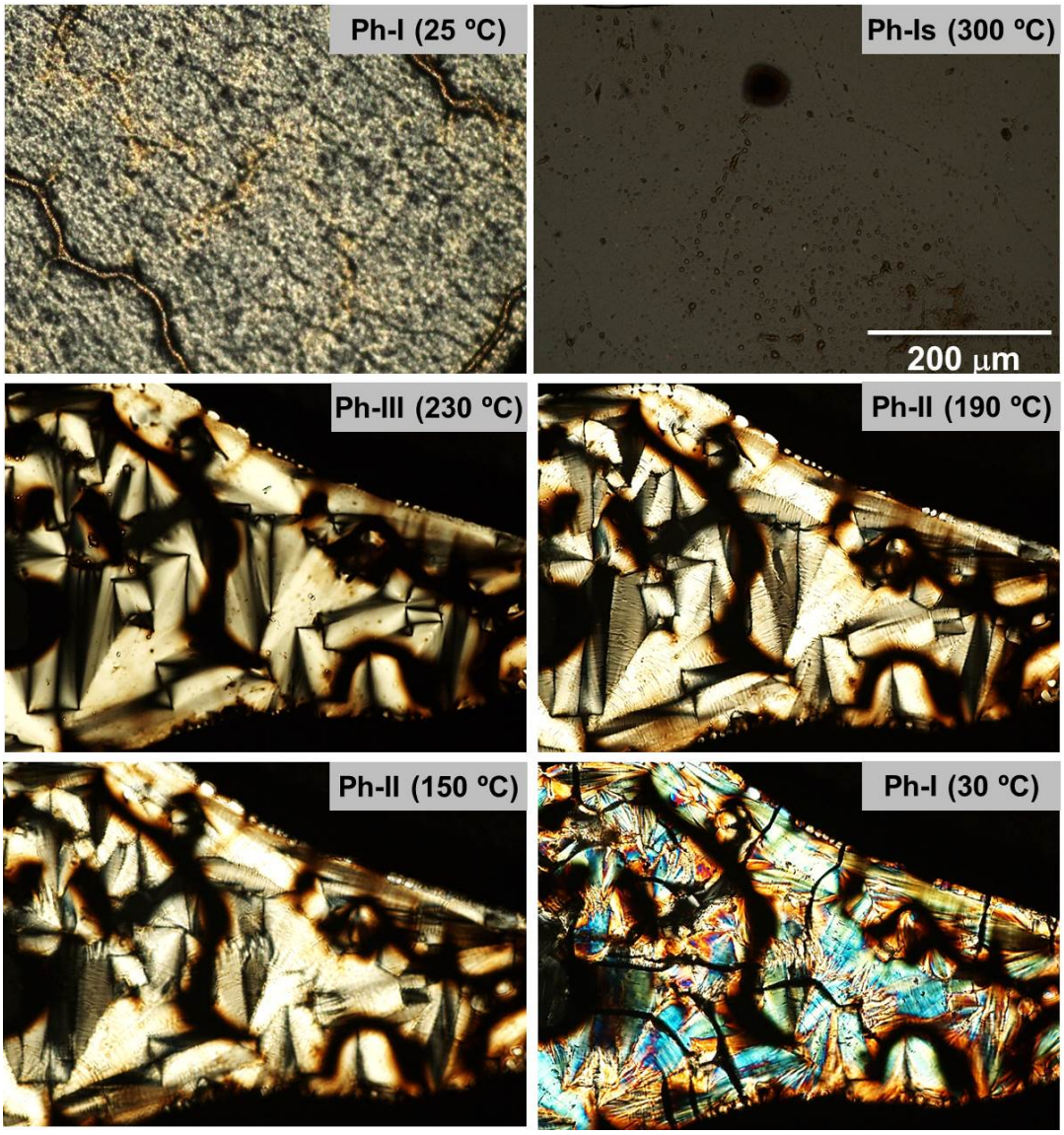

Fig. SI-15. POM micrographs recorded from *n*ATMP·Br at the indicated temperatures.

Tables

Table SI-1. Crystal data and structure refinement for 12ATMP·Br.

Empirical formula	C_{15} H_{34} Br P
Formula weight	325.30
Temperature	293(2) K
Wavelength	0.071073 nm
Crystal system, space group	Monoclinic, P 2_1/c
Unit cell dimensions	*a* = 1.82906(10) nm alpha = 90º *b* = 0.79655(4) nm beta = 93.119(2)º *c* = 1.26721(7) nm gamma = 90º
Volume	1843.51(17) $Å^3$
Z, Calculated density	4, 1.172 Mg/m^3
Absorption coefficient	2.301 mm^{-1}
F(000)	696
Crystal size	0.449 x 0.139 x 0.098 mm
Theta range for data collection	2.230 to 25.393º
Limiting indices	-22<=*h*<=22, -9<=*k*<=9, -15<=*l*<=15
Reflections collected / unique	25175 / 3385 [*R*(int) = 0.0429]
Completeness to theta = 25.242	99.9 %
Absorption correction	Semi-empirical from equivalents
Max. and min. transmission	0.7452 and 0.6345
Refinement method	Full-matrix least-squares on F^2
Data / restraints / parameters	3385 /0/169
Goodness-of-fit on F^2	1.046
Final *R* indices [I>2σ (I)]	*R*1 = 0.0298, w*R*2 = 0.0720
R indices (all data)	*R*1 = 0.0480, w*R*2 = 0.0814
Extinction coefficient	n/a
Largest diff. peak and hole	0.329 and -0.255 e.$Å^{-3}$

Table SI-2. Atomic coordinates (x 10^4) and equivalent isotropic displacement parameters ($Å^2$ x 10^3) for 12ATMP·Br. U (eq) is defined as one third of the trace of the orthogonalized Uij tensor.

Atom	x	y	z	U(eq)
Br(1)	1173(1)	830(1)	3176(1)	64(1)
P(1)	1077(1)	9047(1)	6693(1)	44(1)
C(1)	2051(1)	8920(3)	6601(2)	53(1)
C(2)	2286(1)	8825(3)	5469(2)	53(1)
C(3)	3109(1)	8874(3)	5373(2)	52(1)
C(4)	3318(1)	8836(3)	4230(2)	53(1)
C(5)	4135(1)	8870(3)	4091(2)	54(1)
C(6)	4340(1)	8855(3)	2952(2)	52(1)
C(7)	5158(1)	8870(3)	2808(2)	54(1)
C(8)	5366(1)	8861(3)	1673(2)	55(1)
C(9)	6188(1)	8880(3)	1543(2)	56(1)
C(10)	6405(1)	8870(3)	408(2)	58(1)
C(11)	7220(2)	8917(3)	286(2)	68(1)
C(12)	7431(2)	8903(4)	-854(3)	96(1)
C(1A)	735(1)	10919(3)	6096(2)	57(1)
C(1B)	654(1)	7295(3)	6042(2)	58(1)
C(1C)	874(2)	9030(4)	8051(2)	60(1)

Table SI-3. Torsion angles (º) for 12ATMP·Br.

C(1A)-P(1)-C(1)-C(2)	-63.2(2)
C(1B)-P(1)-C(1)-C(2)	57.0(2)
C(1C)-P(1)-C(1)-C(2)	176.72(19)
P(1)-C(1)-C(2)-C(3)	174.81(18)
C(1)-C(2)-C(3)-C(4)	-178.1(2)
C(2)-C(3)-C(4)-C(5)	-179.6(2)
C(3)-C(4)-C(5)-C(6)	-179.2(2)
C(4)-C(5)-C(6)-C(7)	-179.4(2)
C(5)-C(6)-C(7)-C(8)	-179.8(2)
C(6)-C(7)-C(8)-C(9)	179.9(2)
C(7)-C(8)-C(9)-C(10)	179.9(2)
C(8)-C(9)-C(10)-C(11)	179.1(2)
C(9)-C(10)-C(11)-C(12)	179.9(2)

Table SI-4. Crystallographic *a* and β values of the *n*ATMP·Br salts used for the simulations of the crystal lattices to obtain their respective SAXS and WAXS profiles.

*n*ATMP·Br	[b]*a* (nm)	β (º)
[a]12	1.83	93.1
14	2.05	97.0
16	2.25	101.0
18	2.47	103.5
20	2.70	106.0
22	2.92	108.0

[a]*a* and β values of 12ATMP·Br are based on the experimental results of 12ATMP·Br.

[b]*b* and *c* parameters and α and γ angles of all the cells are fixed (*b* =0.7965 and *c* = 1.2672 nm, $\alpha = \gamma = 90º$), according to the experimental result of 12ATMP·Br.